Identification of an internal layer in a diffuser

By X. Wu, J. Schluter, P. Moin, H. Pitsch, G. Iaccarino AND Frank Ham

1. Motivation and objectives

Identifying regions of self-preservation in representative non-equilibrium flows is useful for basic fluid mechanics as well as engineering computation. Townsend (1976) discussed the process that sudden changes in external conditions in boundary layers may result in an internal boundary layer that spreads from the section of change, and the layer outside the internal layer develops in almost the same way as in the original flow. Experimental evidence in support of this observation includes the boundary layer over a curved hill (Baskaran *et al.* 1987), and the boundary layer over a bump (Webster *et al.* 1996). In Baskaran *et al.*, streamwise pressure gradient changes rapidly from adverse to favorable at the leading edge, and separation occurs downstream of the summit. Internal layer was found downstream of the leading edge. The flow of Webster *et al.* remains attached, its streamwise pressure gradient changes suddenly from adverse to favorable at both the leading and trailing edges and internal layers were identified downstream of these two locations. They considered signatures of internal layer as knee points in the wall-normal profiles of streamwise turbulence intensity. In these two studies knee points emerge when the outer peak of streamwise turbulence intensity associated with upstream adverse pressure gradient decays rapidly under favorable pressure gradient and an inner peak establishes as a result of the internal layer. Obviously this process of knee point formation is specific to the hill or bump type of flows in which upstream strong adverse pressure gradient changes suddenly to favorable at the leading/trailing edges.

This paper describes an internal layer identified from an incompressible turbulent diffuser flow, as opposed to the internal layers previously identified in external boundary layer flows. The present internal layer emerges in the relaxation zone downstream of a sharp variation in streamwise pressure gradient: from mildly favorable to strongly adverse, then weakly adverse. Unlike those in Baskaran *et al.* and Webster *et al.*, the present internal layer does not display significant spreading into the central region of the flow. The flow in the region where internal layer forms exhibits certain characteristics similar to those observed the C-type of Couette-Poisuille turbulent flows.

Two laboratory incompressible diffuser flows have emerged in a number of fundamental and modeling studies on spatially developing complex internal turbulent flows, namely, the Azad diffuser (Azad 1996) and the Obi diffuser (Obi *et al.* 1993). The Azad diffuser is an axisymmetric conical geometry with a total divergence angle of 8° and with fully developed pipe flow at the inlet. The inlet Reynolds number based on friction velocity and pipe diameter is 12,400. Extensive measurements have been performed on this flow by Okwuobi & Azad (1973), Trupp *et al.* (1986) and Azad & Kassab (1989), among others. They found that sudden application of adverse pressure gradient at the diffuser throat affects the flow so drastically that the downstream mean and turbulent fields become unrecognizable in relation to the inlet condition. The Obi diffuser has an asymmetric planar configuration with a total expansion ratio of 4.7 and a single sided deflection wall

of 10°, see figure 1. The inlet was designed to be a fully developed turbulent channel flow, though in some of the experiments this condition was not achieved. The inlet Reynolds number based on friction velocity and channel half height is 500. Obi *et al.* (1993) studied the flow experimentally using a single component laser-Doppler anemometer. Buice & Eaton (1997) made hot-wire and pulsed-wire measurements in the Obi diffuser. Lindren *et al.* (2002) made measurements on a slightly modified geometry based on the Obi diffuser at a higher Reynolds number to study the control of flow separation. Lim & Choi (2004) performed shape optimization using the Obi diffuser as the base flow configuration. The Obi diffuser has also been used as a test flow in a number of computational studies. These include the Reynolds-averaged simulation of Durbin (1995) and Iaccarino (2001), as well as the large eddy simulation work of Kaltenbach *et al.* (1999). Previous investigations in the Azad diffuser emphasized the process of instantaneous flow reversal (Azad 1996): note that their time-averaged flow is not separated. Likewise, work in the Obi diffuser emphasized the unsteady process of separation on the lower deflected wall, e.g., see Kaltenbach *et al.* (1999). The focus of the present study is on the discovery of an internal layer over the upper flat wall of the Obi diffuser, a subject that has eluded attention in the previous diffuser studies which have focused on separation and reattachment over the lower deflected wall.

Aside from the obvious outstanding issue of identifying internal layers in internal flows, further flow physics questions can be raised with reference to the conditions under which internal layers may form, and the statistical and structural features of the internal layer, as well as possible connection between turbulent fluctuations inside internal layer and identifiable large scale motions in the central region of the flow. In addition, from the view point of basic fluid mechanics it is of interest to query whether it is possible to relate the characteristics of internal layer with any well-known fundamental equilibrium component flows. Furthermore, the original process described by Townsend (1976) needs further scrutiny: Does the layer outside the internal layer develop as in the original unperturbed flow? Does the internal layer emerge right at the streamwise section of change? In this work we attempt to address these flow physics questions using large eddy simulation.

2. Computational details

We consider incompressible fluid flow with constant density ρ in the Obi planar diffuser shown in figure 1. Unit length scale is h, the inlet channel half-height. The two transitional curvatures between the parallel walls and the inclined wall have the same radius of 19.4. The origin of the coordinate system is at the intersection of the deflected wall and the lower inlet channel wall. The curvature center associated with the upstream curved section is located at ($x = -1.7$, $y = -19.4$). The curvature center of the downstream curved section is at ($x = 43.7$, $y = 12.0$). The inlet plane is located at $x = -5$, and the outlet plane at $x = 100$. Spanwise dimension of the computational domain is $8h$.

Unit velocity scale is defined as the friction velocity u^* at the inlet. This then defines the unit time scale as $h/u^*_{x=-5}$. Reynolds number Re based on the unit length h and unit velocity $u^*_{x=-5}$ is 500. As in previous studies of the Obi diffuser, e.g., Buice & Eaton (1997) and Kaltenbach *et al.* (1999), the majority of the results to be presented in this paper were normalized by the inlet bulk velocity u_b defined as the area-averaged mean streamwise velocity at the $x = -5$ station.

The numerical methodology used to solve the filtered continuity and momentum equa-

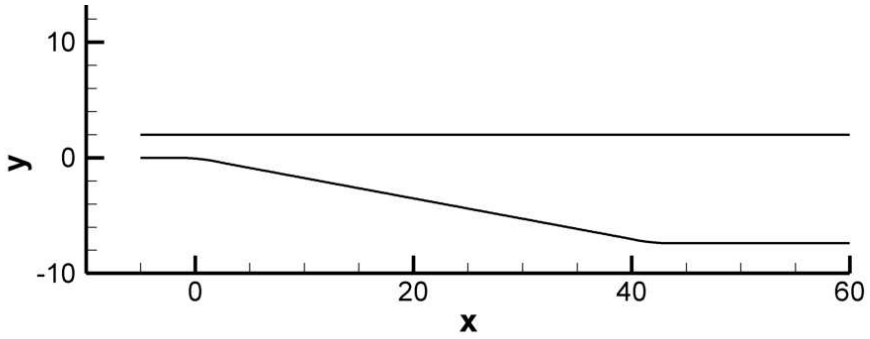

FIGURE 1. Cross-section of the asymmetric planar diffuser; the exit is at $x = 100$.

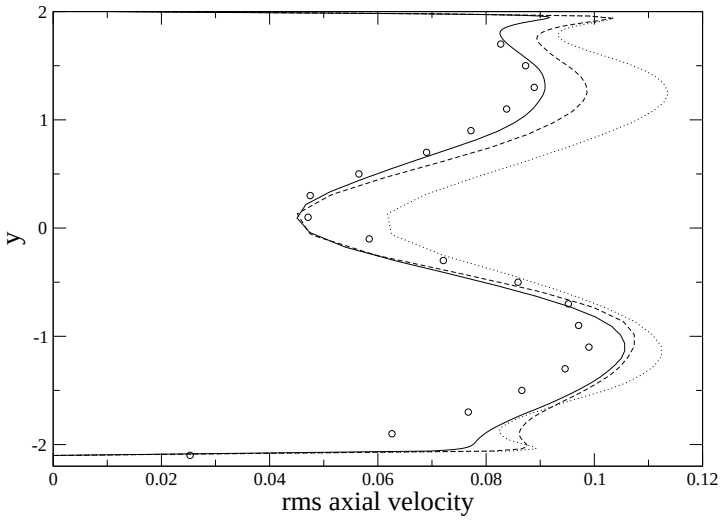

FIGURE 2. $\overline{u}'_{rms}/u_b$ versus y at $x = 11.96$ showing the effects of resolution and subgrid scale model on LES results. ∘ Buice & Eaton (1997); solid line: fine resolution; dashed line: coarse resolution; dotted line: coarse resolution without subgrid scale model.

tions is the unstructured fractional step method for large eddy simulation in complex geometries of Mahesh *et al.* (2004) with the dynamic subgrid-scale procedure of Germano *et al.* (1991). Velocities at the inflow boundary plane, $x = -5$, are from a separate LES of fully developed channel flow at $Re = 500$. Simulations were performed on two sets of hexahedral meshes. The fine mesh has $590(x) \times 100(y) \times 110(z)$ control volume cells. The coarse mesh has $360(x) \times 80(y) \times 80(z)$ control volume cells. Figure 2 shows the effects of grid resolution and subgrid-scale stress model on predicted rms velocity at $x = 11.96$.

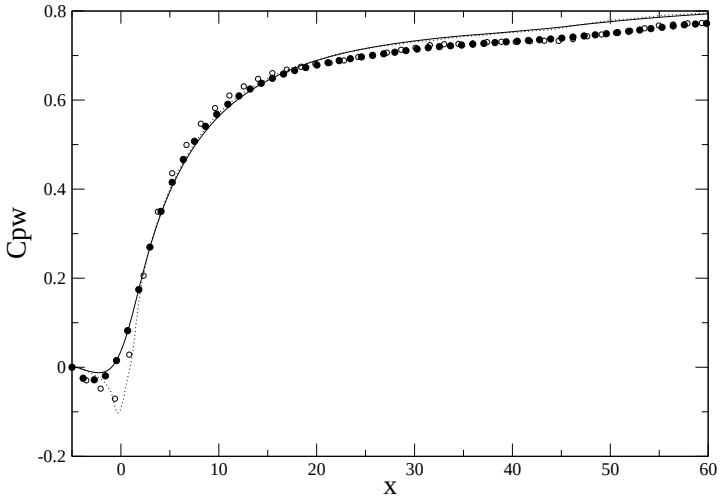

FIGURE 3. Wall static pressure coefficient C_{pw}. Kaltenbach *et al.* (1999): ∘ (lower wall); • (upper wall). Present LES: dotted line (lower wall); solid line (upper wall).

3. Results and discussion

Planar and conical diffusers have broadly similar wall static pressure distributions. A mildly favorable pressure gradient turns to sharply adverse at the diffuser throat, followed by a gradual decrease in the magnitude of adverse pressure gradient further downstream. Such similarity can be appreciated by comparing the C_{pw} results for the Obi diffuser in figure 3 with figure 4 of Okwuobi & Azad (1973) for the axisymmetric Azad diffuser. In figure 3 the change from strongly adverse to weakly adverse pressure gradient starts near $x = 10$, and in Okwuobi & Azad (1973) similar transition takes place approximately 8 pipe radii downstream of the throat, though the leveling off of C_{pw} is not as distinct as in the Obi diffuser. This pattern of C_{pw} for incompressible diffuser flows may be contrasted with the behavior of C_{pw} found in the hill/bump flows of Baskaran *et al.* (1987) and Webster *et al.* (1996). In Webster *et al.* there are two adverse to favorable pressure gradient changes where signatures of internal layers emerge. The magnitude of their favorable pressure gradient decreases further downstream of the trailing edge. The diffuser flow and the bump flow both experience sharp variation in streamwise pressure gradient followed by downstream relaxation. The difference is that the signs of the sudden changes are opposite. Given the fact that internal layer exists in the scenario where C_{pw} is from adverse to favorable, a query which naturally presents itself is whether internal layer can be found in the other scenario.

Skin friction coefficient C_f over the upper flat wall in the Obi diffuser displays a long plateau extending from $x = 15$ to 45 (figure 4). The plateau is bound by a sharp drop from $x = 0$ to 10 upstream and a more gradual decline downstream of $x = 45$. In the plateau region, friction velocity is approximately 0.43, and 1 viscous wall unit corresponds to $0.0047h$. Broadly similar streamwise variation of C_f exists in the Azad diffuser, see figure 17 of Azad (1996). Though in his flow the sharp drop of C_f near the diffuser throat is followed by an additional slower decrease rather than a distinct plateau. In Webster *et al.* (1996) two sudden jumps in C_f are found at the locations where pressure gradient

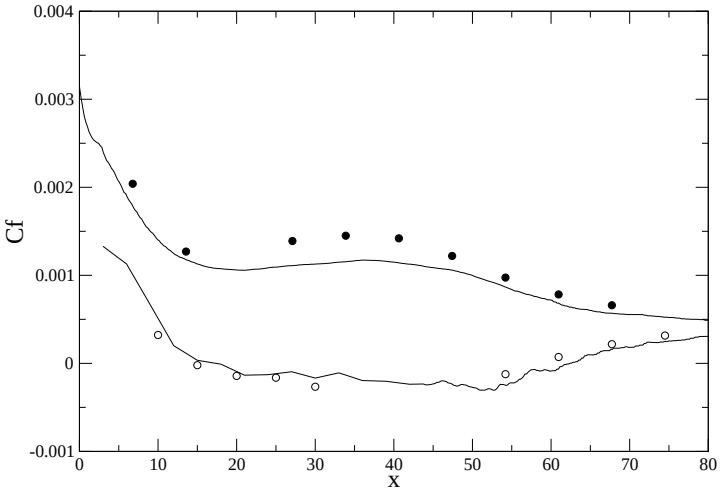

FIGURE 4. Skin friction coefficients. Buice & Eaton (1997): ∘ lower wall, • upper flat wall; solid lines are from the present LES.

changes from adverse to favorable. Downstream of their trailing edge C_f settles into a minor descending slope and signature of internal layer is distinct in this region. Abrupt increase in C_f implies quasi-step changes in the near-wall mean velocity gradient. Thus, production terms which are directly dependent on this gradient in the transport equations for second-order turbulence statistics will be expected to show large increases in the near-wall region, for example, streamwise intensity. The argument that a quasi-step increase in C_f selectively modifies near-wall shear production of turbulent stresses and leads to signatures of an internal layer explains well the internal layers identified in Webster *et al.* (1996) and Baskaran *et al.* (1987), but is not directly applicable in the present diffuser flow. This is because near the upper flat wall of Obi diffuser there is no quasi-step increase in C_f. Instead, C_f has a prolonged plateau which is preceded by a rapid decrease. Although the overall trend of C_f in the Obi diffuser is drastically different from that in the Webster bump, both flows nevertheless show regions of stabilized positive skin friction downstream of sections of sudden change. Again, the signs of the sudden changes are opposite. The stabilized C_f in the relaxation region suggests newly established level of near-wall mean velocity gradient, which may be the driving factor in the formation of an internal layer. Obviously if the sharp drop in C_f on the upper wall of the Obi diffuser is severe enough to cause separation there can be no internal layer. It is expected that internal layer, if it does exist in the Obi diffuser, will be less pronounced than that in the bump flow of Webster *et al.* (1996).

The newly established level of near-wall mean velocity gradient after sudden change implied by figure 4 can be more directly seen from figure 5 and figure 6 in which $\langle\overline{u}\rangle/u_b$ at a number of x stations is plotted against the y coordinate. Experimental data of Buice & Eaton (1997) and Obi *et al.* (1993) are also shown for comparison. For example in figure 6 the near-wall slope of $\langle\overline{u}\rangle/u_b$ decreases from $x = 6.4$ to 10.4, remains nearly constant from $x = 18.4$ to 38.4, and decreases further from $x = 42.4$ to 58.4. The mean velocity distributions are consistent with the sharp drop in C_f followed by a prolonged

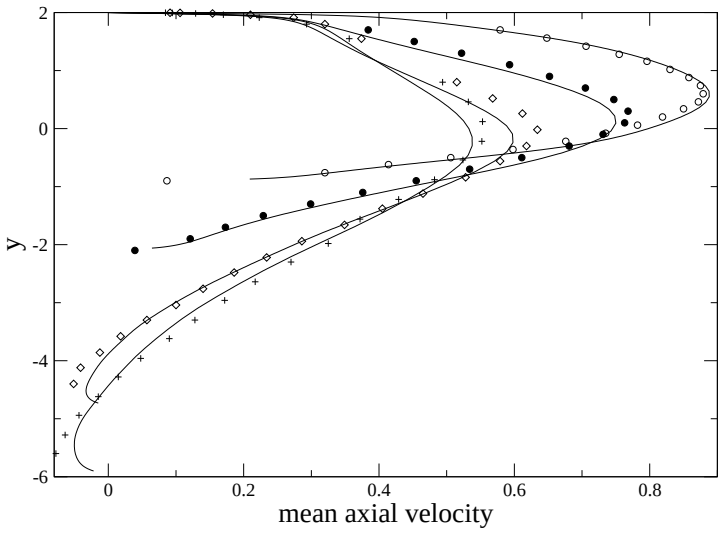

FIGURE 5. $\langle\overline{u}\rangle/u_b$ versus y. Symbols are from Buice & Eaton (1997) and lines are present LES. $\circ$ $x = 5.18$, $\bullet$ $x = 11.96$, $\diamond$ $x = 27.1$, $+$ $x = 33.86$.

plateau spanning from $x = 15$ to 45 shown in figure 4. On the scales adopted in the figures, mean velocity profiles near the top flat wall exhibits nearly discontinuous abrupt change of curvature at $y \approx 1.8$ for those streamwise stations located within the range from $x = 11.96$ to 38.4. In addition, along the wall-normal direction from the abrupt change to approximately $y = 0$, $\langle\overline{u}\rangle/u_b$ displays linear slopes at these streamwise stations. In this paper we will refer this region as the flow outside the internal layer, the outer flow, or the core region. The linearity of mean velocity in the core region is significant because it implies that the velocity difference is only a function (not necessarily linear) of distance to the wall for the outer flow, thereby satisfying a crucial condition in Millikan's reasoning for the existence of logarithmic velocity profile in the overlap region for the flow underneath the core flow. Based on the results of figure 4, figure 5 and figure 6, we can predict that in the C_f plateau region underneath the core flow the mean velocity profiles are logarithmic.

The above prediction is put to test in figure 7 by plotting the mean velocity $\langle\overline{u}\rangle^+$ against wall distance $(2-y)^+$ using wall units. Using the friction velocity suggested in figure 4 it can be shown that $y = 1.8$ corresponds to approximately 45 wall units at each of the selected five x locations. From $(2-y)^+ = 20$ to 80 the $\langle\overline{u}\rangle^+$ profiles at these five streamwise stations collapse onto a logarithmic curve with the well-known slope of $1/0.4$. Very close to the wall $(2-y)^+ < 10$ the usual Law of the Wall is satisfied. We consider one of the properties of the present internal layer is that the mean velocity obeys self-similar Log Law and Law of the Wall inside the internal layer, and varies linearly with distance from the wall outside the internal layer. It may be possible to further collapse the $\langle\overline{u}\rangle/u_b$ profiles at different streamwise locations outside the internal layer in the core region of the flow. For scaling of mean velocity in adverse pressure gradient boundary layers, see the work of Na & Moin (1998) and references therein. Scaling in simple equilibrium internal flows was discussed in a recent paper of Nakabayashi *et al.* (2004).

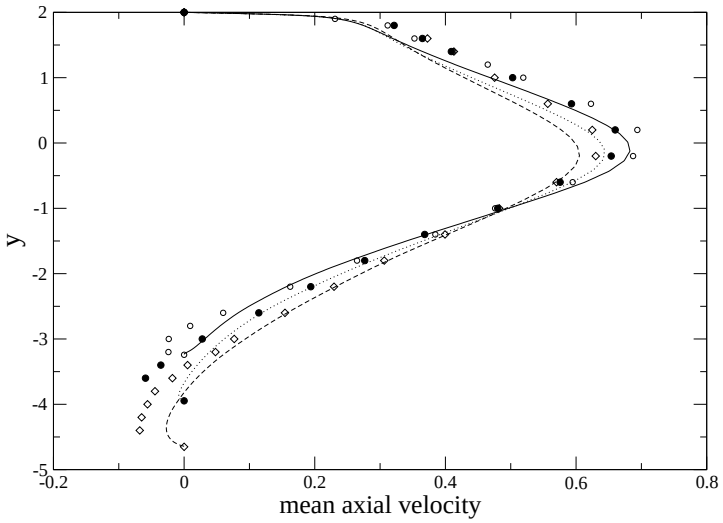

FIGURE 6. $\langle\overline{u}\rangle/u_b$ versus y. Symbols are from Obi *et al.* (1993) and lines are present LES. $\circ$ solid $x = 18.4$, $\bullet$ dotted $x = 22.4$, $\diamond$ dashed $x = 26.4$.

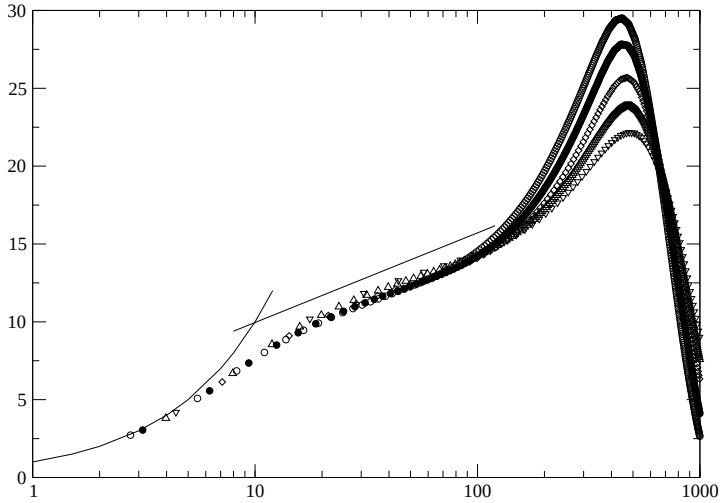

FIGURE 7. $(2-y)^+$ versus $\langle\overline{u}\rangle^+$. $\circ$ $x = 18.4$, $\bullet$ $x = 22.4$, $\diamond$ $x = 26.4$, $\triangle$ $x = 30.4$, $\triangledown$ $x = 34.4$; solid lines are $\langle\overline{u}\rangle^+ = y^+$ and $\langle\overline{u}\rangle^+ = 2.5 \ln y^+ + 4.2$.

Mean streamwise velocity and its wall-normal gradient near the top wall at $x = 20$ are presented in figure 8. In the region of $1 < y < 2$ and $18 < x < 38$ the present mean velocity profiles exhibit similar characteristics to those in the C-type of Couette-Poiseuille turbulent flows measured by Nakabayashi *et al.*, compare figure 8 with the sketch shown in figure 9. The inflectional point where second-order wall-normal mean

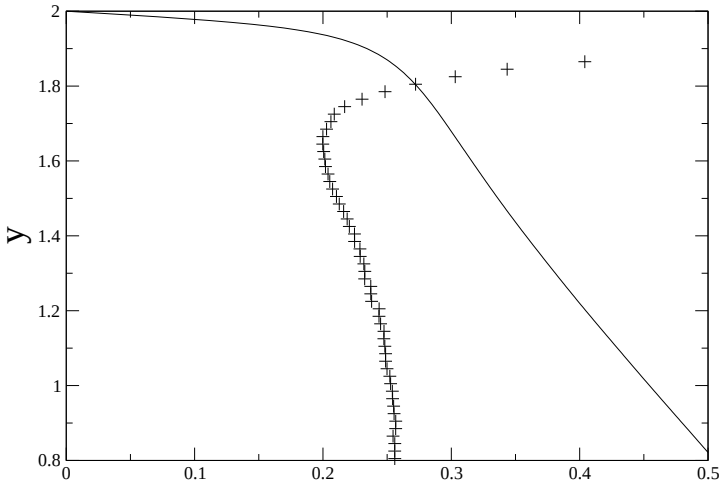

FIGURE 8. Mean velocity and its wall-normal gradient versus y near the top wall at $x = 20$. Solid line: $\langle\overline{u}\rangle/u_b$; +: $-1/u_b\partial\langle\overline{u}\rangle/\partial y$.

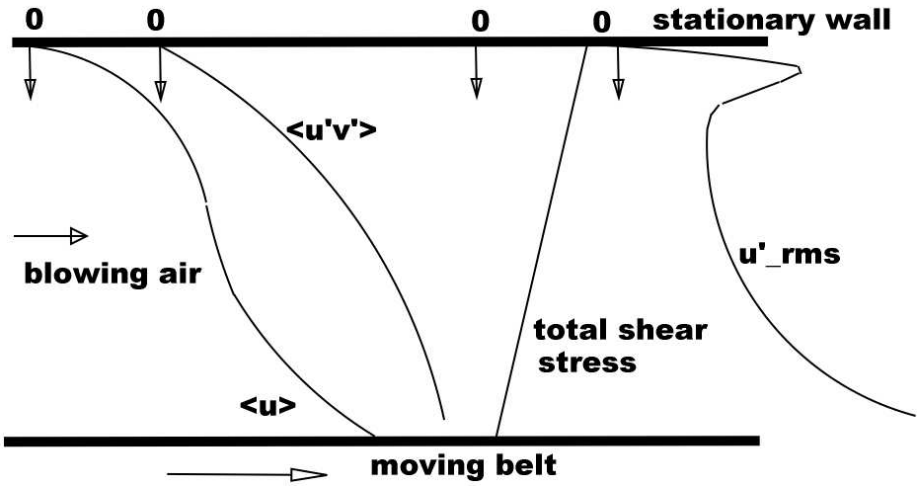

FIGURE 9. Sketch of the C-type of Couette-Poiseuille turbulent flows, following the experimental data of Nakabayashi *et al.* (2004).

velocity gradient changes sign is less apparent from the distribution of $\langle\overline{u}\rangle/u_b$ in the present diffuser flow compared to that indicated by figure 9 for the C-type of flow. However the profile of $\partial\langle\overline{u}\rangle/\partial y$ shown in figure 8 clearly demonstrates that the inflection is located at approximately $y = 1.7$. The effect on mean velocity of the lower moving wall in the C-type of flow is accomplished in the present diffuser flow by the high speed fluid beyond the core region, i.e., $y < 1$. Thus if the C-type of Couette-Poiseuille turbulent flows can be considered approximately as a distant prototype in the region of $1 < y < 2$

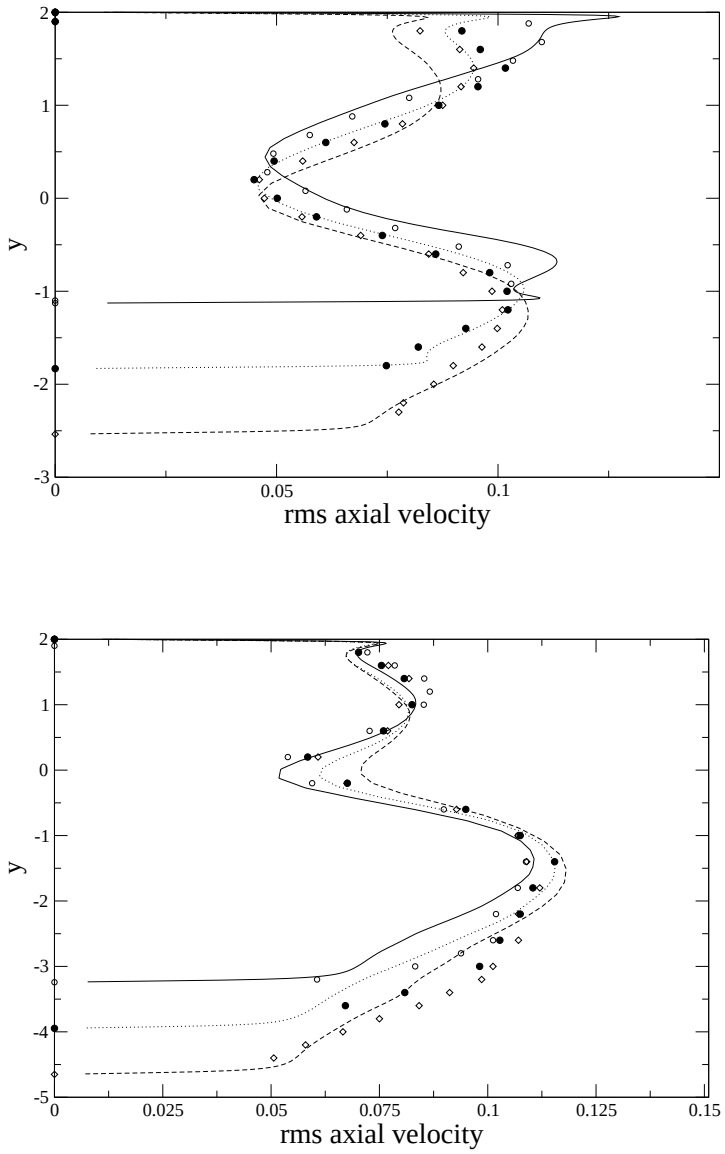

FIGURE 10. $\overline{u}'_{rms}/u_b$ versus y. Symbols are from Obi *et al.* (1993) and lines are present LES. Upper: ∘ solid $x = 6.4$, • dotted $x = 10.4$, ⋄ dashed $x = 14.4$; Lower: ∘ solid $x = 18.4$, • dotted $x = 22.4$, ⋄ dashed $x = 26.4$.

and $18 < x < 38$, the linearly varying high speed fluid flow away from the top wall is then one of the driving components in the internal layer formation process because it provides the necessary mechanism for mean velocity inflection in this particular flow.

In the flow over a bump of Webster *et al.* (1996), prior to the sudden change of C_{pw} near the trailing edge the level of u'_{rms} is elevated and its peak displaced away from the

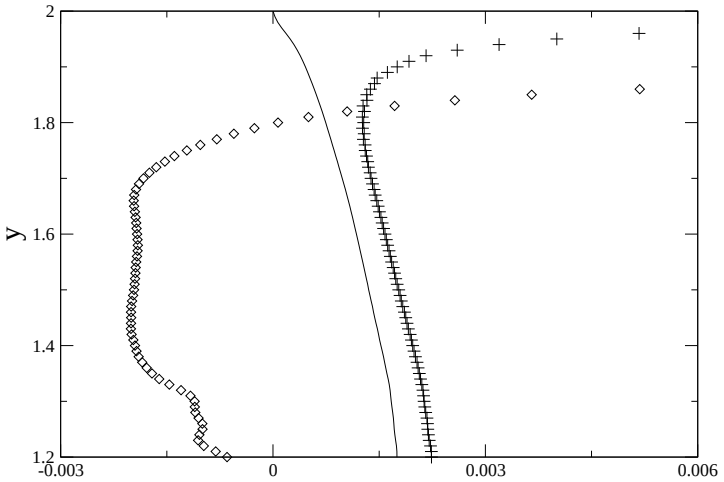

FIGURE 11. Shear stress and its wall-normal gradient versus y near the top wall at $x = 20$. Solid line: Reynolds shear stress $\langle \overline{u}' \overline{v}' \rangle / u_b^2$; +: total shear stress $\langle \overline{u}' \overline{v}' \rangle / u_b^2 - 1/Re u_b \partial \langle \overline{u} \rangle / \partial y$; $\diamond$: wall-normal gradient of total shear stress.

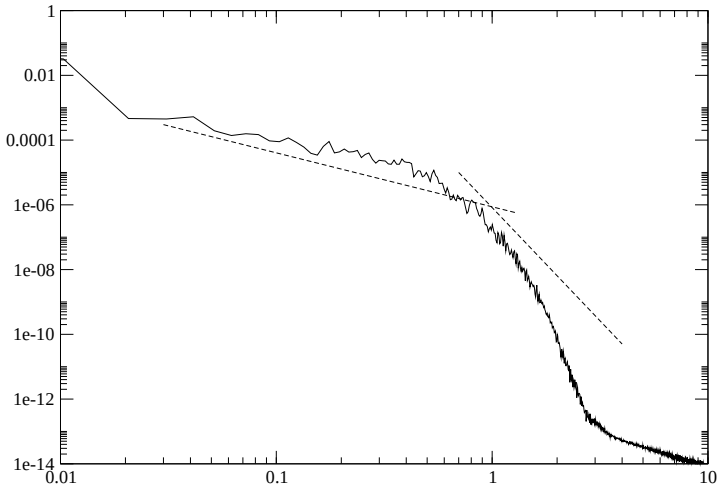

FIGURE 12. Periodogram estimator of frequency spectrum E_{11}/u_b^2 as a function of f/u_b at $x = 30$, $y = 1.8$ and $z = 1$. The left and right dashed lines represent the $-5/3$ and -7 slopes, respectively.

wall to the central region of the boundary layer. As the streamwise pressure gradient changes from adverse to favorable an inner peak of u'_{rms} appears while the outer peak due to upstream adverse pressure gradient diminishes rapidly under the effect of newly imposed favorable pressure gradient so that the wall-normal profiles of u'_{rms} show knee points, i.e., sharp turning, at the edge of internal layer. Sudden application of strong

adverse pressure gradient at the throat of the Obi diffuser significantly elevates $\overline{u}'_{rms}$ near the upper flat wall, the local peak value at the throat is nearly 100% larger than the inlet peak. But this elevated peak decays rapidly back to the original inlet peak level by $x = 10$ as a result of the leveling off of C_{pw} shown in figure 3. This process of rise and decay corresponds to the precipitous drop and subsequent stabilization in C_f discussed in figure 4. Under the effect of adverse pressure gradient, the elevated $\overline{u}'_{rms}$ in the region away form the wall bifurcates away from the inner peak and forms an outer peak. This outer peak is the one commonly observed when boundary layer responds to adverse pressure gradient. It shifts away from the wall with increasing streamwise distance from $x = 6.4$ to 14.4. This process can be discerned from figure 10. Because the flow is still under the influence of weak adverse pressure gradient downstream of $x = 10$ the outer peak does not decay as quickly as in Baskaran *et al.* and Webster *et al.*. Thus, in the Obi diffuser, internal layer signatures may also include a valley bottom at $y \approx 1.8$ separating the inner and outer peaks. The streamwise range within which such a signature is distinct is from $x = 15$ to 40, consistent with figure 7. Comparison of the computed turbulence intensity with experimental data further downstream of the last x station in figure 10 is less satisfactory; this is very similar to findings from Kaltenbach *et al.* (1999) and the other computational studies of the Obi diffuser. Kaltenbach *et al.* commented that the data of Obi *et al.* (1993) downstream of $x = 40$ are only of qualitative value for validation because of a possible scaling problem. No inflectional points can be found in the Reynolds shear stress and wall-normal intensity profiles.

The notion that the present internal layer together with its surrounding environment bears certain resemblance to the fundamental C-type of Couette-Poiseuille turbulent flows is reinforced by considering the characteristics of second-order turbulence statistics in these two flows. The $\overline{u}'_{rms}$ profiles close to the top wall in figure 10 bear remarkable resemblance to those shown in figure 14 of Nakabayashi *et al.* (2004). The valley between the inner and outer peaks in the present discussion is termed as plateau region by Nakabayashi *et al.*. Reynolds shear stress similarity between these two types of flows can be appreciated by comparing the $\langle u'v' \rangle$ profile in figure 11 with those in figure 4 of Nakabayashi *et al* (2004). Note the absence of inflection in the Reynolds shear stress profiles for both flows. Apparently, the total shear stress in the present diffuser flow at $x = 20$ close to the top wall has different behavior from that in the C-type of Couette-Poiseuille turbulent flows. This reflects the fact that the present flow is not one-dimensional and fully developed as assumed in the C-type of Couette-Poiseuille turbulent flows. The wall-normal gradient of total shear stress shown in figure 11 also serves as a measure for identification of internal layer. In adverse pressure gradient boundary layer flows it is approximately equal to the streamwise gradient of total pressure. Outside the internal layer the total pressure on a streamline continues to change slowly as in the upstream flow, whereas inside the internal layer under adverse pressure gradient the total pressure increase along a streamline, being equal at the wall to the static pressure. In the present flow the location at which the total shear stress gradient changes sign serves as one the markers for the edge of the internal layer.

Velocity signals were recorded at selected points for a duration of 32,000 time steps. The raw records were processed using the data windowing technique of Press *et al.*. (1992). The computed periodogram estimator of the power spectrum with data windowing E_{11}/u_b^2 is presented in figure 12. Normalization follows convention so that the spectrum axis has a dimension of unit length h, and the horizontal frequency axis has a dimension of h^{-1}. The extent within which the slope of E_{11} agrees with the $-5/3$ inertial

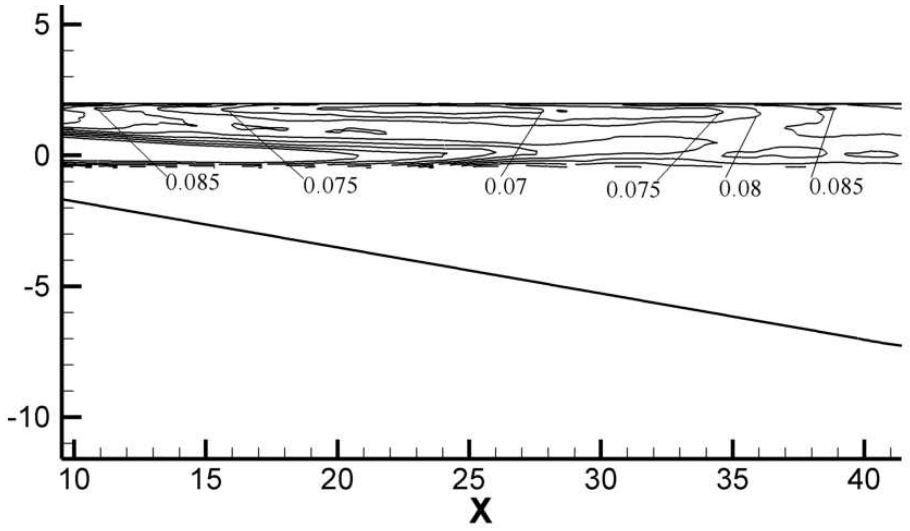

FIGURE 13. Visualization of the internal layer using contours of rms axial turbulence intensity.

subrange law is impressive. In addition, a modest extent of -7 slope is also evident. Grid spacing limits the highest frequency that can be locally resolved in the simulation, and this represents an implicit filter that is imposed by the grid on the flow field (Mittal & Moin 1997). Based on the streamwise grid spacing and the local value of mean streamwise velocity $\langle\overline{u}\rangle$, the normalized Nyquist critical frequency f_c/u_b is approximately 1.2. Spectrum results at higher frequencies may therefore be ignored on the figure.

The internal layer itself is visualized in figure 13 using contours of rms axial turbulence intensity. An imaginary nearly horizontal line connecting the local tips of the contours close to the top wall can be considered approximately as the outer edge of the internal layer.

4. Conclusions

In the concluding remarks of Azad & Kassab (1989), it was commented that *"it may also be conjectured that there is a new growth of a layer in the diffuser wall underneath the retarded, fully developed flow coming from the pipe into the diffuser"*. Our results near the upper wall region of the asymmetric planar Obi diffuser supports their conjecture, albeit at a much lower Reynolds number and also with qualifications.

The new layer is identified as an internal layer but with slow growth. Mean streamwise velocity possesses a well-defined logarithmic slope inside the internal layer until 80 wall units, and varies linearly with wall-normal distance outside the internal layer. One of the statistical indicators of an internal layer is inflectional characteristic in the wall-normal profile of streamwise turbulence intensity. This may take the concrete form of knee-point as reported in the external flow over a hill (Baskaran *et al.* 1987), or valley as found in the present internal flow through a planar diffuser. Internal layers have a tendency to emerge in the relaxation zone downstream of a sudden change in streamwise pressure gradient. Examples of such abrupt change in pressure gradient include the adverse to favorable drop at the trailing edge of the bump of Webster *et al.* (1996), as well as the favorable to adverse jump at the throat regions of the Azad diffuser (Okwuobi & Azad 1973) and the

Obi diffuser. Obviously one prerequisite for internal layer formation is that the abrupt change in pressure gradient may not lead to flow separation, though instantaneous flow reversal is not precluded. We argue that it is possible to relate the occurrence of internal layer to the skin-friction coefficient C_f, which is directly related to the near-wall mean velocity gradient. For instance, a step increase in C_f is found after the trailing edge of the Webster bump corresponding to the adverse to favorable streamwise pressure gradient transition, followed by a gradual leveling off. Over the upper wall of the Obi diffuser, a rapid drop in C_f corresponding to the favorable to adverse pressure gradient jump is followed by a leveling off downstream of $x = 15$. The establishment and stabilization of a new level of C_f signals the birth of internal layer and may be considered as an indicator.

Approximately speaking, the present internal layer and the outer flow associated with it together constitute a distant analogue to the fundamental C-type of Couette-Poiseuille turbulent flows studied recently by Nakabayashi *et al.* (2004). They share broadly similar characteristics of mean and second-order turbulence statistics, but the total shear stress profiles are distinctly different. The role of the lower moving wall in the C-type flow is substituted by the high speed fluid in the central region of the diffuser where the mean velocity $\langle\overline{u}\rangle$ varies linearly with wall-normal coordinate. In this sense the linearly varying high speed flow in the outer region provides the necessary mean flow inflection mechanism for the fluid close to the wall, and may be regarded as one of the driving components in the present internal layer process. The location at which the total shear stress gradient changes sign serves as one the markers for the edge of the internal layer.

Clarifications should be added with reference to the discussion of Townsend (1976) that sudden changes in external conditions in boundary layers may result in an internal boundary layer that spreads from the section of change, and the layer outside the internal layer develops in almost the same way as in the original flow. The results from this study suggest that internal layers may emerge in the relaxation zone downstream of a sudden change in streamwise pressure gradient. Furthermore, the layer outside the internal layer does not behave as if it were unperturbed, i.e., in the same way as in the original flow. On the contrary the flow outside the internal layer displays distinct relaxation characteristics consistent with the removal of strong pressure gradient. Admittedly such observations are limited to the internal layers arising from sudden changes in streamwise pressure gradient. Other perturbation mechanisms, e.g., change in surface roughness, probably will result in an internal layer process not entirely the same as described in this paper.

Acknowledgments

Discussions with Juan Alonso, Sourabh Apte, Peter Bradshaw, George Constantinescu, Massimiliano Fatica, Sangho Kim, Krishnan Mahesh and Cliff Wall are acknowledged. This work is supported by the Advanced Scientific Computing program of the United States Department of Energy. The simulations were performed on the IBM terascale parallel machines at San Diego Supercomputing Center and at Lawrence Livermore National Laboratory.

REFERENCES

Azad, R.S. 1996, Turbulent flow in a conical diffuser: a review. *Experimental Thermal and Fluid Science* **13**, 318–337. Special issue for Peter Bradshaw 60th birthday.

AZAD, R.S. & KASSAB, S.Z. 1989, Turbulent flow in a conical diffuser: overview and implications. *Phys. Fluids* **A1**, 564–573.

BASKARAN, V., SMITS, A.J. & JOUBERT, P.N. 1987, A turbulent flow over a curved hill. Part 1. Growth of an internal boundary layer. *J. Fluid Mech.* **182**, 47–83.

BUICE, C.U. & EATON, J.K. 1997, Experimental investigation of flow through an asymmetric plane diffuser. *Ph.D. Thesis*, Department of Mechanical Engineering, Stanford University.

DURBIN, P.A. 1995, Separated flow computations with the $k-\epsilon-v^2$ model. *AIAA J.* **33**, 659–664.

GERMANO, M., PIOMELLI, U., MOIN, P. & CABOT, W.H. 1991, A dynamic subgrid-scale eddy viscosity model. *Phys. Fluids A* **3**, 1760–1765.

IACCARINO, G. 2001, Prediction of a turbulent separated flow using commercial CFD codes. *J. Fluids Eng.* **123**, 819–828.

KALTENBACH, H.J., FATICA, M., MITTAL, R., LUND, T.S. & MOIN, P. 1999, Study of flow in a planar asymmetric diffuser using large eddy simulation. *J. Fluid Mech.* **390**, 151–185.

LIM, S. & CHOI, H. 2004, Optimal shape design of a two-dimensional asymmetric diffuser in turbulent flow. *AIAA J.* **42**, 1154–1169.

LINDGREN, B., TORNBLOM, O. & JOHANSSON, A.V. 2002, Flow facility design and experimental studies of wall-bounded turbulent shear flows. *Ph.D. Thesis*, Royal Institute of Technology, Stockholm, Sweden.

MAHESH, K., CONSTANTINESCU, G. & MOIN, P. 2004, A numerical method for large eddy simulation in complex geometries. *J. Comp. Phys.* **197**, 215–240.

MITTAL, R. & MOIN, P. 1997, Suitability of upwind biased finite difference schemes for large eddy simulation of turbulent flows. *AIAA J.* **35**, 1415–1417.

NA, Y. & MOIN, P. 1998, Direct numerical simulation of a separated turbulent boundary layer. *J. Fluid Mech.* **370**, 175–202.

NAKABAYASHI, K., KITOH, O. & KATOH, Y. 2004, Similarity laws of velocity profiles and turbulence characteristics of Couette-Poiseuille turbulent flows. *J. Fluid Mech.* **507**, 43–69.

OBI, S., AOKI, K. & MASUDA, S. 1993, Experimental and computational study of turbulent separating flow in an asymmetric plane diffuser. *Ninth Symp. Turbulent Shear Flows, Kyoto, Japan, August 16-19.*

OKWUOBI, P.A.C. & AZAD, R.S. 1973, Turbulence in a conical diffuser with fully developed flow at entry. *J. Fluid Mech.* **57**, 603–622.

PIERCE, C.D. & MOIN, P. 2004, Progress variable approach for large-eddy simulation of non-premixed turbulent combustion. *J. Fluid Mech.* **504**, 73–97.

PRESS, W.H., TEUKOLSKY, S.A., VETTERLING, W.T. & FLANNERY, B.P. 1992, *Numerical Recipes in FORTRAN.* Cambridge University Press.

TOWNSEND, A.A. 1976 *The Structure of Turbulent Shear Flow.* Cambridge University Press.

TRUPP, A.C., AZAD, R.S. & KASSAB, S.Z. 1986 Near wall velocity distributions within a straight conical diffuser. *Experiments in Fluids* **4**, 319–331.

WEBSTER, D., DEGRAAFF, D. & EATON, J.K. 1996 Turbulence characteristics of a boundary layer over a two-dimensional bump. *J. Fluid Mech.* **320**, 53–69.